A template-proximal RNA paired element contributes to *Saccharomyces cerevisiae* telomerase activity

ANITA G. SETO,[1] KFIR UMANSKY,[3] YEHUDA TZFATI,[3,4] ARTHUR J. ZAUG,[1,2] ELIZABETH H. BLACKBURN,[4] and THOMAS R. CECH[1,2]

[1]Department of Chemistry and Biochemistry, and [2]Howard Hughes Medical Institute, University of Colorado, Boulder, Colorado 80309-0215, USA
[3]Department of Genetics, Silberman Institute of Life Sciences, The Hebrew University of Jerusalem, 91904 Jerusalem, Israel
[4]Department of Biochemistry and Biophysics, University of California, San Francisco, San Francisco, California 94143-2200, USA

ABSTRACT

The ribonucleoprotein complex telomerase is critical for replenishing chromosome-end sequence during eukaryotic DNA replication. The template for the addition of telomeric repeats is provided by the RNA component of telomerase. However, in budding yeast, little is known about the structure and function of most of the remainder of the telomerase RNA. Here, we report the identification of a paired element located immediately 5′ of the template region in the *Saccharomyces cerevisiae* telomerase RNA. Mutations disrupting or replacing the helical element showed that this structure, but not its exact nucleotide sequence, is important for telomerase function in vivo and in vitro. Biochemical characterization of a paired element mutant showed that the mutant generated longer products and incorporated noncognate nucleotides. Sequencing of in vivo synthesized telomeres from this mutant showed that DNA synthesis proceeded beyond the normal template. Thus, the *S. cerevisiae* element resembles a similar element found in *Kluyveromyces* budding yeasts with respect to a function in template boundary specification. In addition, the in vitro activity of the paired element mutant indicates that the RNA element has additional functions in enzyme processivity and in directing template usage by telomerase.

Keywords: Ribonucleoprotein; secondary structure; telomerase; template; yeast

INTRODUCTION

Telomerase, the chromosome end-replicating enzyme, contains an RNA subunit essential for its function (Greider and Blackburn 1987). The RNA provides the template for the synthesis of telomeric repeat sequences by the catalytic reverse transcriptase (Blackburn 2000). Telomerase is found in most eukaryotes, and the catalytic protein subunit (TERT) has been shown to have high sequence conservation among divergent organisms (Kelleher et al. 2002). The RNA subunit, on the other hand, shows little primary sequence conservation, even between closely related species. Furthermore, the length of telomerase RNAs varies greatly among eukaryotes: 150–200 nt for ciliated protozoa, 300–500 nt for vertebrates, and >1 kb for budding yeasts. Despite the apparent lack of conservation, we are beginning to elucidate important functional regions of these RNAs.

Phylogenetic analysis has greatly aided the understanding of telomerase RNA secondary structure in ciliates and vertebrates (Romero and Blackburn 1991; Lingner et al. 1994; McCormick-Graham and Romero 1995; Chen et al. 2000). In these two classes of organisms, a large phylogeny of sequences and relatively short RNAs facilitated comparative sequence analysis, leading to conserved core secondary structure predictions. These two core structures have striking similarities to each other, demonstrating that despite primary sequence divergence and differences in length, the important structural determinants of telomerase RNA function may in actuality be quite similar (Chen et al. 2000).

Secondary structure determination for yeast telomerase RNAs has been more challenging, primarily because of their longer lengths and the small pool of known yeast RNA sequences. However, some functional elements have been determined for the *Saccharomyces cerevisiae* RNA. An Sm-protein-binding site was found to be critical for RNA maturation and stability (Seto et al. 1999). Through genetic approaches, a stem–loop structure was shown to be important for interaction with the DNA repair protein Ku (Peterson et al. 2001). Deletion analysis revealed that about half of the

RNA was dispensable for in vivo function, and coimmunoprecipitation studies showed that distinct regions for binding two different protein subunits reside within the essential region (Livengood et al. 2002).

Through the cloning and sequencing of four additional *Kluyveromyces* species budding yeasts, followed by sequence comparison with *Kluyveromyces lactis*, a conserved paired element adjacent to the template was found. Biochemical and genetic analyses showed that the element specifies a template boundary (Tzfati et al. 2000). Cloning of additional *Kluyveromyces* species sequences allowed comparison of telomerase RNAs from six *Kluyveromyces* species, which uncovered seven highly conserved regions, two of which form a pseudoknot element that is essential for telomerase function (Tzfati et al. 2003). Comparison of these RNAs with the telomerase RNA from *S. cerevisiae* revealed a conserved bulged-stem structure that is important for interaction with *S. cerevisiae* Est1p, a telomerase regulatory subunit (Seto et al. 2002).

In addition to the Est1p-binding bulged stem, we now report that a template-proximal paired element is also conserved between the *Kluyveromyces* species and *S. cerevisiae*. Mutagenesis of this structure showed that it is important for telomerase function in vivo and in vitro. Sequencing of telomeres from mutant strains showed that disruption of the paired element can result in read-through beyond the template, or an alteration in usage of sequence within the template. Furthermore, mutants of this paired element have aberrant in vitro telomerase polymerization activity, implying functions of the element beyond serving as a template boundary.

RESULTS

Identification and characterization of a putative template-proximal paired element in *S. cerevisiae* telomerase RNA

To identify potential secondary structures in *S. cerevisiae* telomerase RNA (*TLC1* RNA), the 5′ region of the RNA was subjected to the computer folding program RNA mfold (Zuker et al. 1999). A 7-bp helical structure was predicted to form immediately 5′ of the template region (boldface in Fig. 1A). A similar element was previously identified in *Kluyveromyces* telomerase RNAs, and shown to be important for specification of the template boundary (Tzfati et al. 2000). The putative paired element in *S. cerevisiae* shares characteristics with the *Kluyveromyces* element, in that the pairing spans >300 nt and is almost immediately adjacent to the template (Fig. 1A). As shown in Figure 1A, the predicted paired element is located in a position where it could delimit the extent of primer extension by telomerase, perhaps by forming a simple physical barrier to elongation.

To test the importance of the putative paired element in
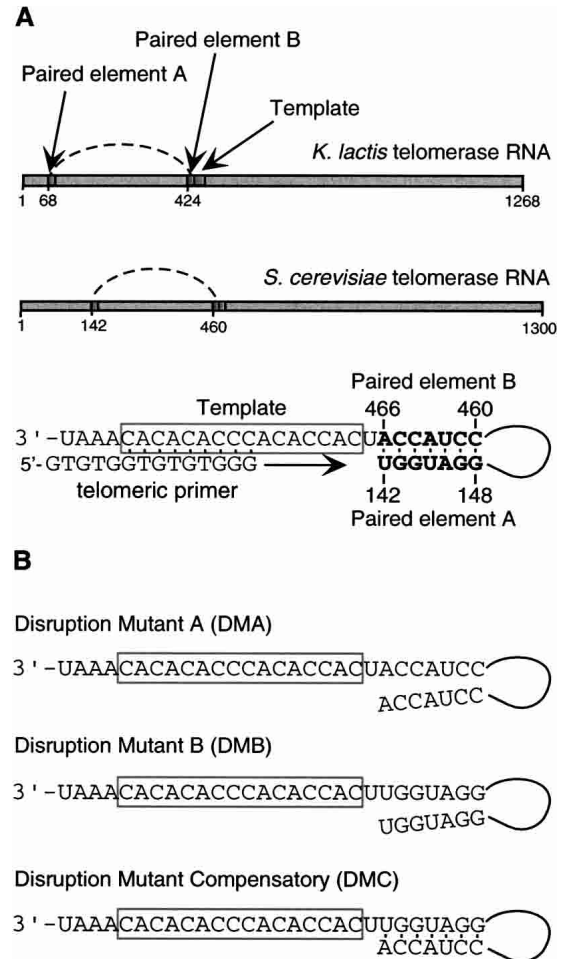
FIGURE 1. A conserved template-proximal paired element in telomerase RNAs from budding yeasts. (*A*) A paired element located 5′ of the template region of *Saccharomyces cerevisiae* telomerase RNA was found by computer folding prediction. This long-range interaction is comprised of pairing between *S. cerevisiae* nucleotides 142–148 and 460–466 and resembles a similar element found in *Kluyveromyces lactis* telomerase RNA. (*B*) Mutations made in the *S. cerevisiae* telomerase RNA to test the predicted template-proximal paired element. Mutations were constructed in a *CEN* low-copy expression vector with *TLC1* RNA expression driven from its endogenous promoter. Disruption Mutant A (DMA) replaced the sequence of paired element A with the sequence of paired element B. Disruption Mutant B (DMB) replaced the sequence of paired element B with the sequence of paired element A. Disruption Mutant C (DMC) combined the DMA and DMB mutations to restore the pairing potential with a different sequence on both sides of the stem.

S. cerevisiae telomerase function, a series of mutations was designed to disrupt the stem or replace it with a compensatory sequence that restored the pairing potential of the two regions (Fig. 1B). Disruption Mutant A (DMA) replaces the sequence of paired element A with the complementary sequence of paired element B, thereby disrupting the predicted base-pairing between these two elements. Disruption Mutant B (DMB) is similar to DMA in that the putative paired element is disrupted by replacement of the sequence of paired element B with that of paired element A.

Disruption Mutant Compensatory (DMC) contains both DMA and DMB block substitutions, thereby restoring the potential for base-pairing between the two regions while changing the sequence of each side of the helix. Computer folding of these mutants by RNA mfold predicted that the mutants should disrupt or compensate for the pairing as designed (data not shown).

Yeast strains with impaired telomerase undergo telomere shortening, leading to senescence, the eventual cessation of cell population growth. To test the effect of the pairing element mutants on in vivo telomerase function, the mutants were transformed into a *tlc1Δ rad52⁻* strain. The *rad52⁻* strain allowed for clear assessment of defects in telomerase activity by disabling the alternative recombination pathway for telomere maintenance (Lundblad and Blackburn 1993). The complementing *LYS2*-marked *TLC1* plasmid was shuffled out by growth on α-aminoadipate, which is toxic in the presence of the *LYS2* gene product. After loss of the wild-type *TLC1* plasmid, strains containing wild-type *TLC1*, DMA, DMB, DMC, or an empty vector were assayed for growth and telomere length. Colony growth of the DMA, DMB, and DMC strains was indistinguishable from the wild type (Fig. 2A), whereas the empty vector control, as expected, began to senesce 50–75 generations after loss of the wild-type plasmid. Growth of the disruption mutants was assayed for nine restreaks, corresponding to ~225 generations.

Interestingly, despite their wild-type growth phenotype, the DMA and DMB strains had shortened telomeres (Fig. 2B). Telomeres in the DMA and DMB strains appeared to be maintained at a stably shortened length over at least 98 generations (Fig. 2B; only three dilutions shown, corresponding to 42 generations). Presumably this length, which was greater than that seen in the early stages of growth of the control strain lacking telomerase (Fig. 2B, vector lanes), was sufficient to confer wild-type growth. Short telomeres coupled with an absence of growth phenotype have been seen before in strains carrying other mutations in the *S. cerevisiae*

telomerase RNA (Prescott and Blackburn 1997; Seto et al. 1999) or in essential protein components (Friedman and

FIGURE 2. Analysis of growth, telomere lengths, and telomerase RNA levels of pairing element disruption mutants. (*A*) Growth of DMA, DMB, and DMC mutants compared with wild-type *TLC1*. DMA, DMB, DMC, wild-type *TLC1*, and an empty vector were transformed into a *tlc1Δ rad52⁻* strain complemented with wild-type *TLC1* on an *LYS2* plasmid. After loss of the complementing wild-type *TLC1* plasmid by growth on α-aminoadipate, a single colony of each strain was restreaked to selective media. This senescence assay was carried out for nine restreaks, corresponding to ~225 generations. By the ninth restreak (shown), no senescence is observed. (*B*) Telomere length analysis of DMA, DMB, and DMC mutants compared with wild-type and empty vector. Strains were generated as described for *A*. After loss of the complementing wild-type *TLC1* plasmid, a single colony was picked into liquid culture, diluted 200-fold, then regrown to saturation. Four successive serial dilutions were performed. Genomic DNA was prepared from each saturated culture, corresponding to ~42 generations in total, digested with *Xho*I to release terminal telomeric restriction fragments, resolved on an agarose gel, and analyzed by Southern blotting with probes to telomeric sequence and a region of Chromosome IV (chr IV). The markers shown were radiolabeled φX174-*Hae*III-digested DNA fragments. (*C*) Telomerase RNA levels of DMA, DMB, and DMC mutants. Single colonies of DMA, DMB, DMC, and wild-type *TLC1* were picked into liquid culture and serially diluted seven times, as described for *B*, corresponding to ~98 generations of growth. Total RNA was prepared from these cultures and separated on a 4% PAGE-7 M urea gel and Northern blotted; RNAs were visualized by hybridization with random-primed DNA probes to full-length *TLC1* and U1 RNAs. Telomerase RNA levels were quantitated by PhosphorImager analysis. The *TLC1* RNA signal was normalized to the U1 RNA signal in each lane. The mean of the *TLC1*/U1 ratios for the seven dilutions and its standard deviation are reported below each mutant analyzed.

Cech 1999; Evans and Lundblad 2002). In contrast to the DMA and DMB mutants, the compensatory mutant (DMC) showed wild-type telomere length. Because the combination of two sets of deleterious mutations restored function, these results support the in vivo existence of the computer-predicted paired element. The compensatory mutant demonstrated that formation of the paired element is more important than the absolute sequence of the helix, because the DMC mutant was as effective as wild-type *TLC1* in complementing a *tlc1*Δ strain.

Such severe telomere shortening as seen with DMA and DMB is not typical for block substitutions near the template. Other substitutions that replaced blocks of 4–8 nt in a different *TLC1* region 3′ of the template showed little or no effect on telomere lengths (Seto 2002).

Telomerase RNA levels were assessed to determine whether the mutations in the paired element affected *TLC1* RNA stability (Fig. 2C). Quantitation was performed by normalization of the *TLC1* RNA signal to the U1 small nuclear RNA signal, which was used as an internal standard. Through 98 generations of growth, *TLC1* RNA levels did not show any consistent upward or downward trend. Only the DMB mutation appeared to have a significant effect on *TLC1* RNA levels: Its *TLC1*/U1 ratio was 0.036 ± 0.017, whereas the ratios for wild type (WT) and DMC were 0.096 ± 0.062 and 0.080 ± 0.032, respectively ($p = 0.029$ for DMB compared with WT and $p = 0.007$ for DMB compared with DMC, where p is the probability that two populations are the same with respect to the variable tested, as determined by the Student's t-test). Although the mean value of the *TLC1*:U1 ratio for DMA (0.059 ± 0.029) was lower than that for WT, the difference was not statistically significant ($p = 0.17$). Thus, the approximately twofold reduction in RNA level in the DMB mutant may contribute to its short telomere phenotype.

The substitution of new sequence in an RNA may introduce new structural elements as well as disrupt the targeted element; therefore, we cannot assume that the overall structures of the DMA and DMB RNAs are identical. Structural differences may explain the difference in stability between these mutants.
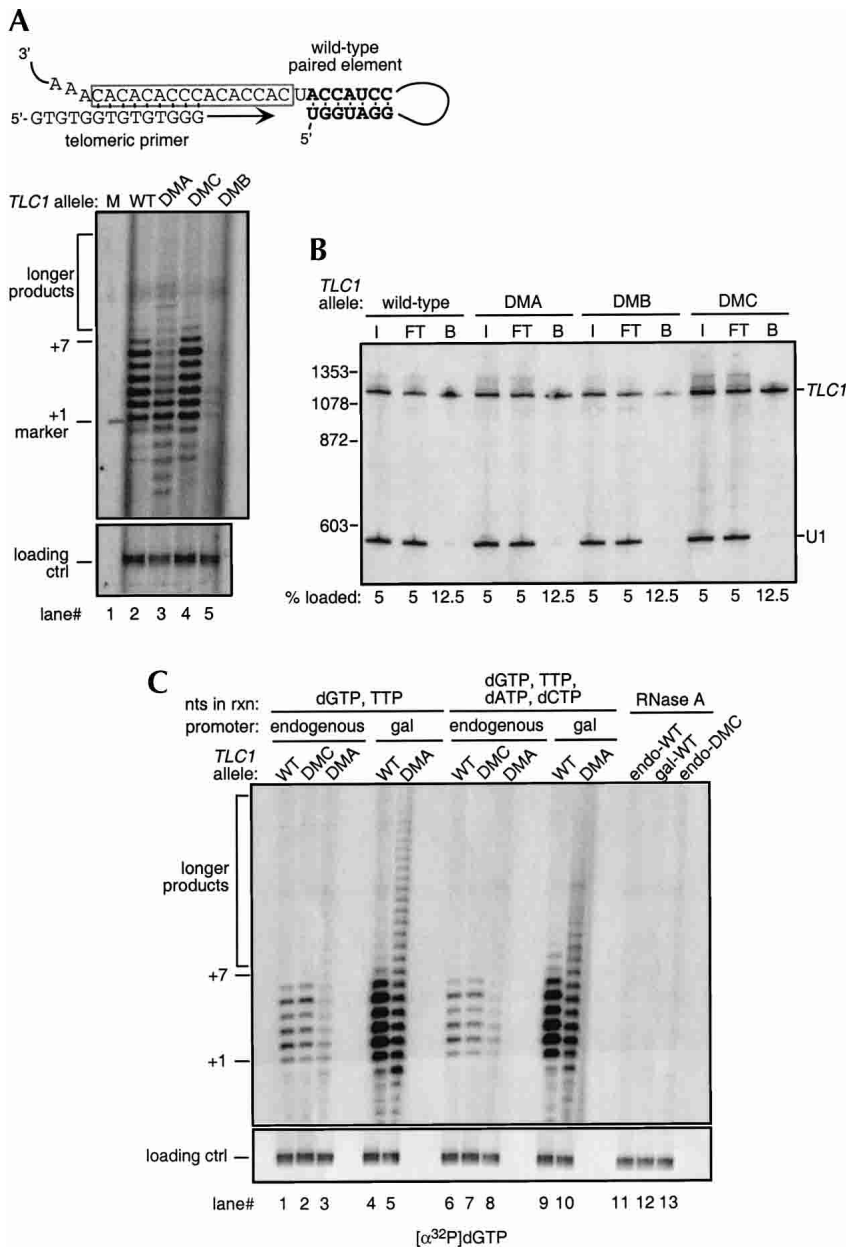
Impaired in vitro activity of paired element mutants

To characterize more directly the effects of paired element mutations on telomerase function, in vitro telomerase activity assays were performed. Telomerase was immunopurified from extracts of strains expressing Protein-A-tagged *EST2* from its endogenous locus and wild-type or mutant *TLC1* RNA from its endogenous promoter on a low-copy *CEN* plasmid. Bead-bound telomerase was incubated with a telomeric oligonucleotide primer, radiolabeled [α-^{32}P]dGTP, and either cold or radiolabeled TTP. The primer extension products were resolved on a polyacrylamide-urea gel. DMC had a level of activity and a pattern of

products similar to those of wild type (Fig. 3A, cf. lanes 2 and 4). DMA and DMB both showed severely reduced levels of in vitro telomerase activity (Fig. 3A, lanes 3,5). The residual pattern of products was RNA-dependent, because preincubation of the beads with RNase A eliminated all activity (Fig. 3C, lanes 11–13; Fig. 4A, lanes 6–7), and is therefore attributed to telomerase rather than some other polymerization activity in the extracts. To visualize DMA products that were comparable in intensity to the weakest wild-type product, twofold to fourfold more immunoprecipitated DMA beads were typically used in the reaction. In vitro activity in the DMB mutant was barely visible above background and was not improved by increasing the amount of extract used in the immunoprecipitation or by optimization of the in vitro assay. Consequently, the in vitro characteristics of this mutant were not further investigated.

The lower in vitro activity of the DMA and DMB mutants could be explained if the mutant RNAs were defective in interaction with the catalytic subunit, Est2p. This possibility was tested by assaying the ability of these RNAs to coimmunoprecipitate with ProA-tagged Est2p. The RNA associated with IgG beads onto which the telomerase complex was immunoprecipitated was analyzed by Northern blotting using probes to *TLC1* and U1 RNAs (Fig. 3B). The DMA and DMC mutants appeared to have little or no difference in coimmunoprecipitation with ProA-Est2p, compared with wild type. The DMB mutant, however, appeared to be less tightly associated with ProA-Est2p. Quantitation of three independent experiments showed that the signal of DMB bound was $16\% \pm 8.7\%$ of the signal of WT bound. In comparison, the signal of DMA bound was ~95% that of WT bound (from two experiments). Therefore, the weaker association of the DMB mutant may explain the reduced level of in vitro telomerase activity. In contrast, the wild-type level of association of the DMA mutant indicated that the reduction in telomerase activity in this mutant was not caused by a weakened protein–RNA interaction or global misfolding, but rather reflects a deficiency in enzyme function.

The DMA mutant, although severely reduced in the levels of telomerase-extended products, was active enough to allow further in vitro characterization. The DMA mutant had two properties that differed from wild type: longer extension products and a changed pattern of those extension products (Fig. 3A). The longer products were unexpected, because the only nucleotides provided in this experiment were dGTP and TTP, and read-through synthesis should require dATP to copy the next RNA residue following the 5′ boundary of the template (see schematic, Fig. 3A). Therefore, such longer products, rather than being indicative of copying beyond the normal template 5′ boundary as described previously for *K. lactis* telomerase RNA mutants (Tzfati et al. 2000), could either reflect slippage synthesis, resulting in reiterative copying of a portion or portions of the normal template as reported for a template substitution
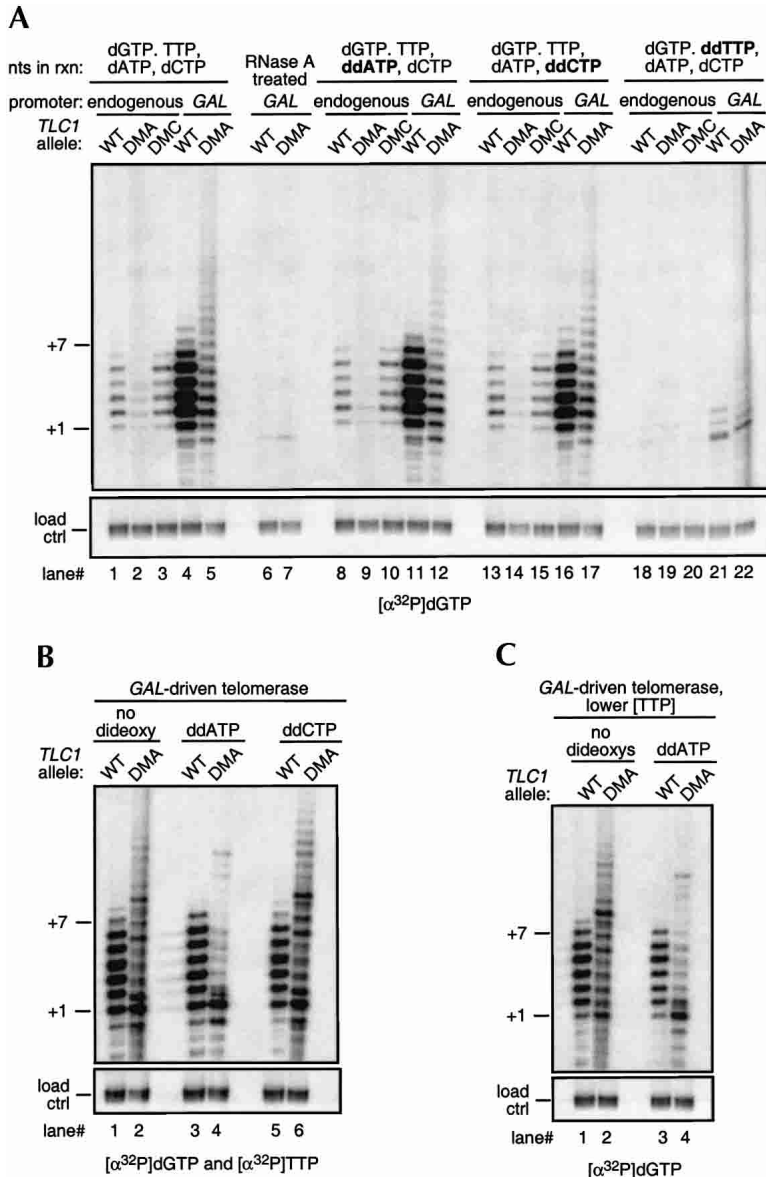
FIGURE 3. In vitro telomerase activity of paired element disruption mutants. (*A*) Telomerase activity immunopurified from wild-type, DMA, DMB, and DMC mutants. Extracts were prepared from a strain expressing ProA-tagged Est2p and wild-type, DMA, DMB, or DMC mutant *TLC1* RNA. Extracts were then incubated with IgG beads to immunopurify telomerase. Beads were assayed for in vitro telomerase activity by incubation with 2.5 μM telomeric primer, 100 μM TTP, and 1.7 μM [α-^{32}P]dGTP, with 5 μL of wild-type beads, 2.5 μL of DMC, and 10 μL each of DMA or DMB beads assayed. Telomerase products were resolved on a 12% PAGE-7 M urea sequencing gel. (Loading ctrl) A control for product recovery: a ^{32}P 5′-end-labeled 100-nt oligonucleotide added immediately after the reactions were stopped and visualized on the same gel. (+1 marker) in lane M was the 14-nt single-stranded telomeric primer extended by 1 nt with the addition of [^{33}P]ddTTP and terminal deoxytransferase. (*B*) Coimmunoprecipitation of telomerase RNA mutants with ProA-Est2p. RNA coimmunoprecipitated with ProA-Est2p on IgG beads was isolated (as described for *A*), and analyzed by Northern blotting (as described for Fig. 2C). Blots were probed with radiolabeled *TLC1* and *U1* gene probes. (I) Input RNA; (FT) flowthrough from beads; (B) RNA bound to beads. The markers shown were radiolabeled ϕX174-*Hae*III-digested DNA fragments. (% loaded) Percentage of input, flowthrough, and bound RNAs loaded onto the gel. (*C*) Telomerase activity in the presence of all four nucleotides, and the effect of overexpression of *TLC1* RNA and ProA-Est2p. Reactions were performed in the absence or presence of both 100 μM dATP and dCTP (lanes *1–5* and *6–10*, respectively). In all cases, reactions contained 100 μM TTP and 0.9 μM [α-^{32}P]dGTP. For the RNase A control reactions, beads were incubated with RNase A prior to the addition of the activity assay components.

mutant of *S. cerevisiae* telomerase RNA (Prescott and Blackburn 1997), or increased processivity, allowing more than one round of template copying. Such multiround processive synthesis in vitro is not normally seen with wild-type yeast telomerase. In addition, the mobility of the products was reproducibly shifted slightly in the DMA mutant; this effect was seen most dramatically beginning at the +6 product and in more highly resolved electrophoresis gels (Fig. 3C, lanes 4,5). Because electrophoretic mobility of oligonucleotides is base-composition-dependent, the altered mobility indicated a different sequence for the DMA product.

Because of the weak activity of the DMA mutant, in vitro analysis of this mutant proved to be very challenging; we therefore constructed a *tlc1Δ* strain in which both *ProA-EST2* and *TLC1* are expressed from a *GAL* promoter on a plasmid. *ProA-EST2* is also expressed from its endogenous locus. It has been previously shown that overexpression of both the RNA and reverse transcriptase components of telomerase results in a significant increase in in vitro activity (Teixeira et al. 2002). When the DMA mutant was overexpressed, we observed a significant boost in levels of in vitro activity (Fig. 3C, cf. lanes 3 and 5). The hallmarks of the DMA mutant—production of longer extension products and the shift in product mobility—were retained and became more obvious in the *GAL*-driven DMA expression strain. The DMB mutant activity was still too weak to allow further characterization (data not shown).

Incorporation of noncognate nucleotides by paired element mutants in vitro

This paired element in *S. cerevisiae* is found in the same location as the *K. lactis* paired element that showed longer extension products in vitro and in vivo, caused by disruption of the helical structure adjacent to the template boundary. We therefore reasoned that the addition of deoxyadenosine might allow the DMA mutant to extend beyond the *S. cerevisiae* template more efficiently, because templating by the sequence beyond the nor-

FIGURE 4. The effect of dideoxynucleotides on in vitro telomerase activity of paired element disruption mutants. (*A*) Activity of bead-bound telomerase in the presence of ddATP, ddCTP, and ddTTP. *CEN-* or *GAL*-expressed telomerase was immunopurified on IgG beads through ProA-Est2p, then assayed for in vitro telomerase activity in the presence of all four nucleotides. (Lanes *8–22*) The corresponding dideoxynucleotide (100 µM) was substituted for the deoxynucleotide. The other deoxynucleotides were present at 100 µM, and [α-^{32}P]dGTP was added at 0.9 µM. The RNase A control reactions were performed as described for Figure 3B. (*B*) The effect of addition of ddTTP on DMA in vitro activity in the presence of [α-^{32}P]dGTP and [α-^{32}P]TTP. *GAL*-driven wild-type and DMA telomerase were immunopurified on IgG beads. Assays were performed in the presence of all four deoxynucleotides (lanes *1,2*), or with ddATP or ddCTP substituting for dATP or dCTP, respectively (lanes *3–6*). In all cases, reactions were performed at 0.9 µM [α-^{32}P]dGTP and [α-^{32}P]TTP, and all other nucleotides were at 100 µM. (*C*) The effect of lowered TTP concentration on DMA in vitro activity. *GAL*-WT and *GAL*-DMA telomerase beads were incubated with 0.9 µM [α-^{32}P]dGTP, 0.9 µM cold TTP, 100 µM dCTP, and 100 µM of dATP or ddATP.

mal template is predicted to require dATP in the absence of misincorporation (see schematic, Fig. 3A). The effect of dCTP was tested simultaneously.

Interestingly, the addition of dATP and dCTP had no apparent effect on the amount of longer extension products, although it did affect the mobility of the products—the +5 and +6 products of lanes 4 and 5 in Figure 3C more closely comigrated than those of lanes 9 and 10, which showed a larger mobility difference (Fig. 3C). This effect was reproducible over three independent experiments. Attempts to PCR-amplify, clone, and sequence the reaction products proved futile, as the excess of unextended primer interfered with the purification of extended products.

To assess whether the DMA mutant incorporated dATP or dCTP in the reaction products, assays were performed in the presence of ddATP or ddCTP. Polymerases cannot extend the dideoxy moiety; therefore, if ddATP or ddCTP is incorporated, shorter products would accumulate through chain termination. In reactions performed in the presence of [^{32}P]dGTP, the indicated dideoxynucleoside triphosphate, and the other two deoxynucleoside triphosphates, we did not observe any effect of the dideoxy (Fig. 4A; e.g., cf. lanes 4, 11, and 16 or lanes 5, 12, and 17). These reactions were repeated in the presence of both [^{32}P]dGTP and [^{32}P]TTP, to increase the intensity of weak bands. Interestingly, under these reaction conditions, we observed a strong accumulation of radiolabeled products at the +1 position in the presence of ddATP in the DMA mutant but not in wild type (Fig. 4B). These results indicated that some DMA products had incorporated a ddA at the +1 position.

At first glance, one may wonder why a primer extended by only cold ddATP would be radiolabeled. However, a yeast telomerase-associated exonuclease has been shown to digest the unextended primer, producing a radiolabeled +0 or shorter primer that will be subsequently extended by telomerase in vitro, resulting in products that are radiolabeled (Niu et al. 2000).

We did not observe the ddATP effect in the presence of only dGTP as the radiolabeled nucleotide, indicating two possibilities: first, the products containing adenosine at the +1 position are not visible unless labeled with [^{32}P]TTP; or second, the 100 µM cold TTP in the reactions shown in Figure 4A suppresses incorporation of ddATP, whereas 0.9 µM [^{32}P]TTP does not. To test the second hypothesis, reactions were performed with 0.9 µM [^{32}P]dGTP, 0.9 µM TTP, and 100 µM dATP or ddATP. As shown in Figure 4C, the ddATP effect of Figure 4B was recapitulated under these reaction conditions. Therefore, it appears that

at high TTP concentrations, the incorporation of ddATP by the DMA mutant is suppressed. Perhaps the DMA mutant has higher affinity for TTP, which is a natural *S. cerevisiae* telomerase substrate, than for ddATP. Thus, in the presence of high TTP concentrations, the enzyme might preferentially misincorporate TTP opposite uridines in the template, at positions where dATP or ddATP would otherwise be added. Alternatively, perhaps a second enzyme activity is dominant at high TTP concentration and masks the activity that would use dATP.

The DMA mutant produced bands at the +6 and +9 positions that were not seen with wild-type telomerase, and that disappeared specifically with ddATP but not ddCTP (Fig. 4B, cf. lanes 2 and 6 with lane 4; Fig. 4C, cf. lanes 2 and 4). In addition to the accumulation of a strong band at the +1 position, the presence of ddATP resulted in a faint pattern of longer extension products that culminate in a longer product at approximately the +11 or +12 position (Fig. 4C, lane 4). This band appears to be telomerase-derived, as it does not appear in the wild-type products; it may reflect a product caused by extension beyond the conventional telomerase RNA template, consistent with our hypothesis that mutation of the paired element would disrupt the ability of the RNA to specify a template boundary. The faint intermediate bands may represent another telomerase activity that does not require dATP.

Sequence analysis of telomeric DNA from pairing element mutant strains

To better understand the in vivo function of the template-proximal paired element, telomeric DNA from each paired element mutants was PCR-amplified, cloned, and sequenced. These sequences were compared with those from the wild-type strain sequenced in parallel. Most of the telomeres isolated from the *CEN*-DMA strain had normal telomeric sequence, although they were very short (24–99 nt for *CEN*-DMA compared with 108–199 nt for WT). However, in four of 13 clones, the telomeres were longer and revealed incorporation of sequence complementary to that of pairing element B (one clone shown in Fig. 5). Read-through of up to 8 nt beyond the normal template was observed. These results indicate that at least some portion of the telomerase enzyme reads beyond the template to incorporate nontelomeric sequence. Interestingly, the long telomeres from the *GAL*-DMA strain had wild-type sequence, showing no incorporation of nontemplate sequence. We do not understand at present how overexpression of the mutant RNA would result in the normal sequence being incorporated.

FIGURE 5. Sequence analysis of telomeric DNA from the DMA mutant reveals incorporation of nucleotides templated by RNA sequence found beyond the normal template. The sequence shown is one of four clones containing read-through sequence. Only the 3′ portion of the telomere is shown in the *bottom* panel. Underlined nucleotides are nontelomeric. Highlighted in red is sequence added from read-through beyond the template.

The telomeres from the DMB mutant also had blocks of aberrant sequence, but these sequences do not appear to result from read-through beyond the template boundary. Instead, long stretches of TG dinucleotides were found at the telomeres of five of 15 *CEN*-DMB clones and nine of 12 *GAL*-DMB clones. These strains had at least eight and up to 26 TG repeats, whereas in wild type, the longest stretch seen was seven repeats. As described in the Discussion, this mutant may use a small portion of the template in a repetitive fashion to generate these repeats.

DISCUSSION

The template-proximal paired element reported here represents the third of only three RNA secondary structure elements that have been experimentally verified for *S. cerevisiae* telomerase RNA. The other two secondary structures are a stem–loop involved in interaction with the Ku protein (Peterson et al. 2001) and a bulged stem necessary for binding the Est1p regulatory subunit of telomerase (Seto et al. 2002). As judged by the growth phenotype observed upon disruption of the template-proximal structure, this element is less important than the Est1p-binding site and comparable in importance to the Ku site. However, the template-proximal paired element directly affects the enzymatic activity of telomerase, whereas deletion of the Ku interaction site did not (Peterson et al. 2001).

The template-proximal paired element in *S. cerevisiae* resembles a similar structure found in *Kluyveromyces* species telomerase RNAs (Tzfati et al. 2000). This structure is also predicted by RNA mfold to form in telomerase RNAs from *Saccharomyces mikatae* and *Saccharomyces bayanus* (D. Zappulla, pers. comm.; sequences kindly provided by Manolis Kellis and Eric Lander, M.I.T.; Kellis et al. 2003). Disruption of this paired element in *K. lactis* resulted in extension

beyond the template boundary, as shown by the dependence of the extension on dATP, the first nontemplate sequence, and other dNTPs expected to be incorporated, as well as sequence analysis of telomeric DNA synthesized in vivo by these mutant telomerases (Tzfati et al. 2000). Disruption of the *S. cerevisiae* paired element also results in the appearance of longer extension products in vitro, and some of these products are likely to be caused by template readthrough, because analysis of telomeric sequence from the *CEN*-DMA strain revealed incorporation of sequence complementary to RNA sequence found beyond the template. However, all of the in vitro products cannot be explained completely by read-through, because the appearance of longer products is not entirely dependent on the presence of dATP. It appears that we are observing overlapping activities of the DMA mutant. In addition to reading beyond the template boundary, the DMA mutant may also generate products through increased processivity from more efficient translocation and/or reiterative copying of a short region within the normal template. The sequencing of in vivo synthesized telomeres from the DMA strain supports this hypothesis: we have observed telomeres containing one full repeat followed by shorter, truncated repeats (Fig. 5).

The sequences of telomeric DNA isolated from the *CEN*-DMA mutant show that read-through is certainly occurring. However, the majority of cloned telomeres do not contain read-through sequences; perhaps most nontelomeric sequence is unstable and subsequently degraded, and there is likely to be selection for survival of yeast whose telomere sequences are normal enough to function in chromosome end protection.

In addition to generating unusually long products in vitro, the DMA mutant also produces short products with shifted mobilities compared to those of wild type. The changed mobility indicates incorporation of a different sequence within the first round of synthesis. A portion of these products disappears with the addition of ddATP at low TTP concentration, indicating that some but not all of the products contain adenosine. We do not know the mechanism of this action, but it is possible that the DMA mutant telomerase sometimes uses a different region of the template to begin synthesis and/or uses a different template sequence entirely. The sequences of the in vivo generated telomeres show no evidence for such an activity, but this may be a difference between in vivo and in vitro enzyme function.

Analysis of telomeres from the DMB mutant reveals unusual incorporation of stretches of TG repeats. One explanation for this observation is that the DMB mutation generated an RNA secondary structure that not only disrupted the template-proximal paired element, but also rearranged the overall structure surrounding the template. This altered structure may render most of the template inaccessible, thereby constraining the reverse transcriptase to the 3′ end

of the template (5′-CACACAC-3′). This result demonstrates that RNA structure is an important determinant for template usage by the telomerase catalytic protein subunit.

Previously, *S. cerevisiae* telomerase RNA mutants that contained triplet nucleotide substitutions in the template region were characterized in vitro (Prescott and Blackburn 1997). Substituting the three nucleotides immediately 5′ of the template (which we predict at least partially disrupts the pairing element) resulted in a strong +8 product, with the dNTP and ddNTP dependencies expected for read-through copying of at least one residue beyond the template sequence. In addition, some products had altered mobilities, compared with products of the wild-type enzyme, similar to what we report here with the DMA mutant.

In summary, the *S. cerevisiae* template-proximal paired element is not essential but contributes to in vivo telomere maintenance. It appears to function by specifying the template boundary, as has been shown for *K. lactis*. In addition, the biochemical characteristics of the paired element mutant indicate that this RNA element may have additional functions in determining enzyme processivity and template sequence usage. Future work should reveal if these functions are provided directly by the RNA or, rather, through its interaction with a protein component such as the Est2p catalytic subunit.

MATERIALS AND METHODS

Plasmid construction

pTLC1-DMA, pTLC1-DMB, and pTLC1-DMC were constructed by introducing the appropriate mutated sequence into pSD107 (*TRP, CEN*, and *TLC1* with endogenous promoter and terminator sequences; Seto et al. 1999). The DMA mutant sequence was inserted by ligation of an *Stu*I–*Nco*I PCR fragment generated with primers bearing the mutated sequence. The DMB mutant was constructed with an *Nco*I–*Hpa*I PCR fragment containing the mutant sequence. DMC was generated by triple ligation of the *Stu*I–*Nco*I DMA and *Nco*I–*Hpa*I DMB fragments into the *Stu*I and *Hpa*I sites of pSD107. pRS314-P_{GAL1}-*TLC1* (*TRP, CEN, GAL-TLC1*) was a gift of J. Lingner, ISREC, Lausanne, Switzerland (Teixeira et al. 2002). pGAL-DMA, pGAL-DMB, and pGAL-DMC were constructed by subcloning the *Bsr*GI to *Not*I fragment from pTLC1-DMA, pTLC1-DMB, or pTLC1-DMC into the corresponding sites in pRS314-P_{GAL1}-*TLC1*. For ProA-Est2p overexpression, *GAL*-pKF412 was constructed by PCR amplification of the *GAL* promoter from pRS314-P_{GAL1}-*TLC1* with flanking *Cla*I restriction sites and subcloned into the *Cla*I site of pKF412 (*URA, 2μ, PROA-EST2*). pKF412 was a gift from K. Friedman, Vanberbilt University. Mutagenesis and DNA manipulations were confirmed by DNA sequencing across the PCR-amplified region.

S. cerevisiae strains and manipulations

TCy43 (Δ*tlc1*∷*LEU2, rad52*∷*LEU2*, pl-TLC1-LYS2-CEN; Seto et al. 1999) or ProA-Est2-*tlc1*∷*LEU2* (containing pRS316/TLC1; Livengood et al. 2002) was transformed with pSD107, pAS500 (empty

vector; Seto et al. 1999), pTLC1-DMA, pTLC1-DMB, pTLC1-DMC, pRS314-P_{GAL1}-*TLC1*, pGAL-DMA, pGAL-DMB, or pGAL-DMC. After growth on selective media, single colonies were picked to α-aminoadipate or 5-FOA, to shuffle out the complementing pTLC1-LYS2-CEN or pRS316/TLC1, respectively. Single colonies were then restreaked to medium lacking tryptophan for further analysis. ProA-Est2-*tlc1*::*LEU2* strains containing pRS314-P_{GAL1}-*TLC1*, pGAL-DMA, pGAL-DMB, or pGAL-DMC were subsequently transformed with *GAL*-pKF412.

Measurements of telomere length

Single colonies from the first restreak on −TRP medium after growth on α-aminoadipate were picked into 5 mL of selective liquid culture. The culture was grown to saturation, then diluted 200-fold to inoculate a fresh 5-mL culture. Saturated cultures were harvested, and genomic DNA was prepared using the DNA-Pure Yeast Genomic Kit (CPG Inc.). Half of the isolated DNA was digested with *Xho*I, resolved on a 1.1% agarose gel, then transferred to Hybond N+ (Amersham Pharmacia) by osmoblotting. DNA was visualized with random-primed radiolabeled probes to telomeric repeat sequences and a fragment of Chromosome IV.

Northern blot analysis of *TLC1* RNA levels

For quantitation of *TLC1* RNA levels over time, 5-mL cultures were grown and diluted as described for telomere length analysis. Total RNA was prepared from cells using hot phenol extraction (Chapon et al. 1997). Approximately 15 μg of total RNA was loaded onto a 4% PAGE-7 M urea gel, then transferred to Hybond N+ (Amersham Pharmacia) by electroblotting. RNAs were analyzed with random-primed probes to the *TLC1* and U1 RNA genes. Quantitation was performed by PhosphorImager analysis using Imagequant software. *P* values were calculated using a Web-based Student's *t*-test program (http://www.physics.csbsju.edu/stats/t-test.html).

Immunoprecipitation of telomerase and coimmunoprecipitation of *TLC1* RNA

Extracts were prepared from ProA-Est2-*tlc1*::*LEU2* strains containing pSD107, pTLC1-DMA, pTLC1-DMB, pTLC1-DMC, pRS314-P_{GAL1}-*TLC1*, pGAL-DMA, pGAL-DMB, or pGAL-DMC as previously described (Livengood et al. 2002), followed by clarification at 16,000g. Extract protein concentrations were determined by Bradford assay. Approximately 1 mg of total protein was added to 20 μL of packed IgG beads (Amersham Pharmacia), then rotated end-over-end at 4°C for 6 h, followed by three washes in extract buffer, followed by two washes in 10 mM Tris-HCl (pH 7.5), 1 mM $MgCl_2$, 10% glycerol, 1 mM DTT, 10 U/mL RNasin (Promega), and 1 mM PMSF. Beads were resuspended in the final wash buffer. To examine coimmunoprecipitation of *TLC1* RNA with ProA-Est2p, RNA bound to IgG beads and from input and flowthrough extracts was isolated as described (Seto et al. 1999). RNA was subjected to Northern blot analysis as described above.

In vitro telomerase activity

Bead-bound telomerase was prepared as described above. Bead supernatant was removed with a Hamilton syringe and incubated with telomerase assay buffer (40 mM Tris-HCl at pH 7.5, 50 mM NaCl, 5% [v/v] glycerol, 0.5 mM spermidine, 0.5 mM DTT, 0.9 μM [α-^{32}P]dGTP, 100 μM TTP, 2.5 mM $MgCl_2$, and 2.5 μM telomeric oligonucleotides) at 30°C for 20 min. For increased signal, 0.9 μM [α-^{32}P]TTP substituted for the cold TTP. Variations to the telomerase assay conditions are described in the text and figure legends. Telomerase extension products were isolated and analyzed as described previously (Seto et al. 1999).

Cloning and sequence analysis of telomere fragments

Genomic DNA was prepared from wild-type, DMA, DMB, and DMC strains, as described (McEachern and Blackburn 1996). DNA was resuspended in TE containing 100 μg/mL DNase-free RNase A and incubated at 37°C for 15 min, followed by phenol:chloroform:isoamylalcohol (25:24:1) extraction, chloroform:isoamylalcohol (24:1) extraction, and ethanol precipitation. The genomic DNA was ligated to an anchor oligonucleotide that was 5′-phosphorylated and 3′-amino-modified to enable the ligation of its 5′ end, but not its 3′ end, to genomic DNA. A typical 20 μL ligation reaction contained 2 μg of genomic DNA, 60 pmole of an anchor oligonucleotide (5′-TTTAGTGAGGGTTAATAAGCGGC CGCGTCGTGACTGGGAGCGC-3′), 50 mM Tris-HCl (pH 8.0), 12.5% PEG 8000, 10 mM $MgCl_2$, 1 mM hexamine cobalt chloride, 20 μM ATP, 10 μg/mL BSA, 1 mM DTT, and 10 units of T4 RNA ligase (New England Biolabs). The reaction was incubated at 37°C for 1.5 h. The ligated DNA was then amplified by PCR using a subtelomeric primer (5′-GTTGCACGGCCGTAGCGAGAG-3′) and a primer complementary to the anchor oligonucleotide (5′-CGACGCGGCCGCTTATTAACCCT-3′). For efficient amplification of the repetitive, G-rich telomeric sequence, a high amount of Taq polymerase and a long extension time were used. Typically, a 40-μL reaction included 100 ng of anchor-primer ligated genomic DNA, 0.5 μM each primer, 0.2 mM each dNTP, 1.5 mM $MgCl_2$, and 3.2 units of Taq polymerase (Bio-X-Act, Bioline GmbH). The amplification cycles included initial denaturation at 94°C for 2 min and 30 cycles of denaturation at 95°C for 30 sec, annealing at 62°C for 45 sec, and extension at 72°C for 120 sec in a T-Gradient thermal cycler (Biometra). The amplified telomere fragments were extracted from an agarose gel, cloned into a TA vector, and sequenced using either M13 universal or M13 reverse primer from the side of the telomeric end (using the G-rich strand as the sequencing template worked best). Sequencing was performed at The Center for Genomic Technologies, Silberman Institute of Life Sciences, The Hebrew University of Jerusalem. For each strain analyzed, 8–15 clones were sequenced. For strains expressing the wild-type and DMC RNAs from either the *CEN* or *GAL* constructs, the average length of telomeric sequence retrieved was similar: 162 bp and 169 bp for *CEN*-WT and *CEN*-DMC, or 182 bp and 214 bp for *GAL*-WT and *GAL*-DMC, respectively. For strains carrying *CEN*-DMA or *CEN*-DMB, the telomeric length was similar to each other and much shorter than that of wild type: 81 bp and 89 bp, respectively. For the *GAL*-DMB strain, the average telomere length was 108 bp, which is significantly shorter than that of wild type or DMC. In contrast, with an average length of 285 bp, the cloned telomeres from the *GAL*-DMA strain were much longer than the *GAL*-WT or *GAL*-DMC lengths. Both wild-type and mutant telomeres showed some minor incorporation of nontelomeric sequence (0–4 nt per telomere), which may be from misincorporation by telomerase or an artifact from the automated

sequence analysis. These nucleotides were disregarded in our analysis.

ACKNOWLEDGMENTS

REFERENCES

Blackburn, E.H. 2000. The end of the (DNA) line. *Nat. Struct. Biol.* **7:** 847–849.

Chapon, C., Cech, T.R., and Zaug, A.J. 1997. Polyadenylation of telomerase RNA in budding yeast. *RNA* **3:** 1337–1351.

Chen, J.-L., Blasco, M.A., and Greider, C.W. 2000. Secondary structure of vertebrate telomerase RNA. *Cell* **100:** 503–514.

Evans, S.K. and Lundblad, V. 2002. The Est1 subunit of *Saccharomyces cerevisiae* telomerase makes multiple contributions to telomere length maintenance. *Genetics* **162:** 1101–1115.

Friedman, K.L. and Cech, T.R. 1999. Essential functions of amino-terminal domains in the yeast telomerase catalytic subunit revealed by selection for viable mutants. *Genes & Dev.* **13:** 2863–2874.

Greider, C.W. and Blackburn, E.H. 1987. The telomere terminal transferase of *Tetrahymena* is a ribonucleoprotein enzyme with two kinds of primer specificity. *Cell* **51:** 887–898.

Kelleher, C., Teixeira, M.T., Forstemann, K., and Lingner, J. 2002. Telomerase: Biochemical considerations for enzyme and substrate. *Trends Biochem. Sci.* **27:** 572–579.

Kellis, M., Patterson, N., Endrizzi, M., Birren, B., and Lander, E.S. 2003. Sequencing and comparison of yeast species to identify genes and regulatory elements. *Nature* **423:** 241–254.

Lingner, J., Hendrick, L.L., and Cech, T.R. 1994. Telomerase RNAs of different ciliates have a common secondary structure and a per-muted template. *Genes & Dev.* **8:** 1984–1998.

Livengood, A.J., Zaug, A.J., and Cech, T.R. 2002. Essential regions of *Saccharomyces cerevisiae* telomerase RNA: Separate elements for Est1p and Est2p interaction. *Mol. Cell. Biol.* **22:** 2366–2374.

Lundblad, V. and Blackburn, E.H. 1993. An alternative pathway for yeast telomere maintenance rescues est1-senescence. *Cell* **73:** 347–360.

McCormick-Graham, M. and Romero, D.P. 1995. Ciliate telomerase RNA structural features. *Nucleic Acids Res.* **23:** 1091–1097.

McEachern, M.J. and Blackburn, E.H. 1996. Cap-prevented recombination between terminal telomeric repeat arrays (telomere CPR) maintains telomeres in *Kluyveromyces lactis* lacking telomerase. *Genes & Dev.* **10:** 1822–1834.

Niu, H., Xia, J., and Lue, N.F. 2000. Characterization of the interaction between the nuclease and reverse transcriptase activity of the yeast telomerase complex. *Mol. Cell. Biol.* **20:** 6806–6815.

Peterson, S.E., Stellwagen, A.E., Diede, S.J., Singer, M.S., Haimberger, Z.W., Johnson, C.O., Tzoneva, M., and Gottschling, D.E. 2001. The function of a stem–loop in telomerase RNA is linked to the DNA repair protein Ku. *Nat. Genet.* **27:** 64–67.

Prescott, J. and Blackburn, E.H. 1997. Telomerase RNA mutations in *Saccharomyces cerevisiae* alter telomerase action and reveal non-processivity in vivo and in vitro. *Genes & Dev.* **11:** 528–540.

Romero, D.P. and Blackburn, E.H. 1991. A conserved secondary structure for telomerase RNA. *Cell* **67:** 343–353.

Seto, A.G. 2002. "Functional elements in the *Saccharomyces cerevisiae* telomerase RNA." Ph.D. thesis, University of Colorado, Boulder, CO.

Seto, A.G., Zaug, A.J., Sobel, S.G., Wolin, S.L., and Cech, T.R. 1999. *Saccharomyces cerevisiae* telomerase is an Sm small nuclear ribonucleoprotein particle. *Nature* **401:** 177–180.

Seto, A.G., Livengood, A.J., Tzfati, Y., Blackburn, E.H., and Cech, T.R. 2002. A bulged stem tethers Est1p to telomerase RNA in budding yeast. *Genes & Dev.* **16:** 2800–2812.

Teixeira, M.T., Förstemann, K., Gasser, S.M., and Lingner, J. 2002. Intracellular trafficking of yeast telomerase components. *EMBO Rep.* **3:** 652–659.

Tzfati, Y., Fulton, T.B., Roy, J., and Blackburn, E.H. 2000. Template boundary in a yeast telomerase specified by RNA structure. *Science* **288:** 863–867.

Tzfati, Y., Knight, Z., Roy, J., and Blackburn, E.H. 2003. A novel pseudoknot element is essential for the action of a yeast telomerase. *Genes & Dev.* **17:** 1779–1788.

Zuker, M., Mathews, D.H., and Turner, D.H. 1999. Algorithms and thermodynamics for RNA secondary structure prediction: A practical guide. In *RNA biochemistry and biotechnology* (eds. J. Barciszewski and B.F.C. Clark), pp. 11–43. Kluwer Academic Publishers, Dordrecht, NL.